

GEOELECTRIC INVESTIGATION OF AWBA EARTH DAM EMBANKMENT, UNIVERSITY OF IBADAN, IBADAN, SOUTHWESTERN NIGERIA, FOR ANOMALOUS SEEPAGES.

Bayowa, O.G.*, Ilufoye, D.T. and Animasaun, A.R.

Department of Earth Sciences, Ladoko Akintola University of Technology, Ogbomosho, Nigeria.

*Corresponding Author:

e-mail: oycbayowa@yahoo.com

(Received: 4th April, 2011; Accepted: 10th September, 2011)

ABSTRACT

A geoelectric investigation involving the Vertical Electrical Sounding (VES), Dipole-Dipole Electrical Horizontal Profiling and Total Field Self Potential (SP) method was carried out along the embankment of Awba Earth Dam constructed within the Precambrian Basement Complex terrain of Southwestern Nigeria. The study was aimed at assessing possible seepage zone(s) under or within the dam embankment. Thirty two VES stations at 10 m interval, were occupied along two 170 m long N-S trending traverses established on the crest of the dam embankment. The VES data were quantitatively interpreted using the partial curve matching technique and 1-D forward modelling with WinResist 1.0 version software. The dipole-dipole data were inverted into 2-D resistivity images using the DIPPRO™ 4.0 inversion software. The SP data were presented as a profile and interpreted qualitatively. Three geoelectric layers were delineated along the two traverses. These include the clay/sandy clay/laterite (cap rock) with layer resistivity and thickness values ranging from 59 - 675 ohm-m and 0.3 - 3.2 m respectively; a clay/sandy clay core/weathered layer with layer resistivity and thickness range of 8 - 166 ohm-m and 3.2 - 53.3 m respectively and a third layer of basement bedrock with layer resistivity values of between 498 and 100000 ohm-m. The 2-D resistivity structure revealed that the core of the dam embankment is characterized by relatively low resistivity zones typical of seepage paths at stations 2 - 3 (20 - 30 m) at about 8 m depth; 4 - 6 (40 - 60 m) and 9 - 11 (90 - 110 m) at a depth range of between 4 and 10 m within the dam embankment along traverse 1. The low resistivity zones were delineated between stations 4 and 6 (40 - 60 m) and 9 and 11 (90 - 110 m) along traverse 2 at depth range of between 0 and 5 m. A major peak negative SP anomaly with amplitudes of about -80 mV and -104 mV on traverses 1 and 2 respectively was delineated between stations 2 and 4 (20 - 40 m). This anomaly is located on a metallic bleeding pipe concealed between the spillway and the dam embankment. The study concluded that the dam embankment contain three suspected seepage zones within / beneath the core.

Keywords: Geoelectric Investigation, Dam Embankment, Anomalous Seepage, University of Ibadan, Nigeria.

INTRODUCTION

All earth dams in their natural state experience some degree of seepage and spillage flow from the reservoir and through permeable soils. Seepage and spillage may also be associated with internal erosion in the dam, and internal erosion is one of the main reasons for dam failures (Sjodahl, 2006). Basement bedrock structures such as faults, joints and fracture zones could also constitute seepage paths from a dam embankment (McLean and Gribble, 1997). Other possible causes of uncontrolled leakage and subsequent dam failure include age of the dam, poor construction material; defect in the design, etc. (Olorunfemi *et al.*, 2000 a and b).

Water movement or seepage through geological formation or engineering structures is amenable to geophysical detection (Bogoslovsky and Ogilvy, 1970; Butler *et al.*, 1988). Electrical resistivity imaging involving the vertical electrical sounding and dipole-dipole arrays is a useful and efficient method for monitoring dam embankment conditions (e.g. Olorunfemi, *et al.*, 2000 a, b and

2004). However, in many cases, the streaming potential resulting from active water flow through hydraulic conduits are readily detectable by the Self Potential (SP) method and hence the geophysical method is commonly used to investigate dam seepage (Haines, 1978; Erchul and Slifer, 1987; Payne and Corwin, 1999). The voltage observable in SP survey can be positive or negative and may amount to some hundreds of millivolts and as such can be observed in conjunction with seepage of water from dams, or the flow of groundwater through different lithological units (Lowrie, 1997). The degree of success in the application of the above geophysical methods however, is a function of the geology and the existence of an electrical resistivity contrast that must be significant and detectable.

In view of the fact that detailed post construction routine check is unavoidable in dam embankment to forestall leakages, this study has employed integrated geophysical investigation involving the VES, dipole-dipole and Total Field SP methods to

image the Awba Earth Dam Embankment in order to investigate possible spurious seepage (s). The integrated approach is usually preferred for such investigation so as to improve the quality of interpretation as this may compensate for the ambiguity inherent in the use of a single geophysical method and thus improve the resolution of the imaging of subsurface structure(s) (Christensen and Sorensen, 1994).

Location and Characteristics of the Dam Site

The Awba earth dam whose volume of the earth fill is 38 000 m³ is located within the campus of the University of Ibadan (UI), Ibadan, Southwestern

Nigeria (Fig.1). The dam lies within Longitudes 03°52.85' and 03°54.12' E and Latitudes 07°26.85' and 07°27.50' N. It sources its water from streams emanating from River Eleyele which also sources its water from River Ona within Ibadan metropolis. The dam embankment is 110 m long, 8.5 m high while the width of its crest is 12 m (Fig. 2). Its surface area is about 81 sq. km. The reservoir level is 5 m and the length of the pool is 700 m. Awba dam is designed to impound about 227 million litres of water. It is accessible through the Wadie Martins road within the University Campus (Fig. 3).

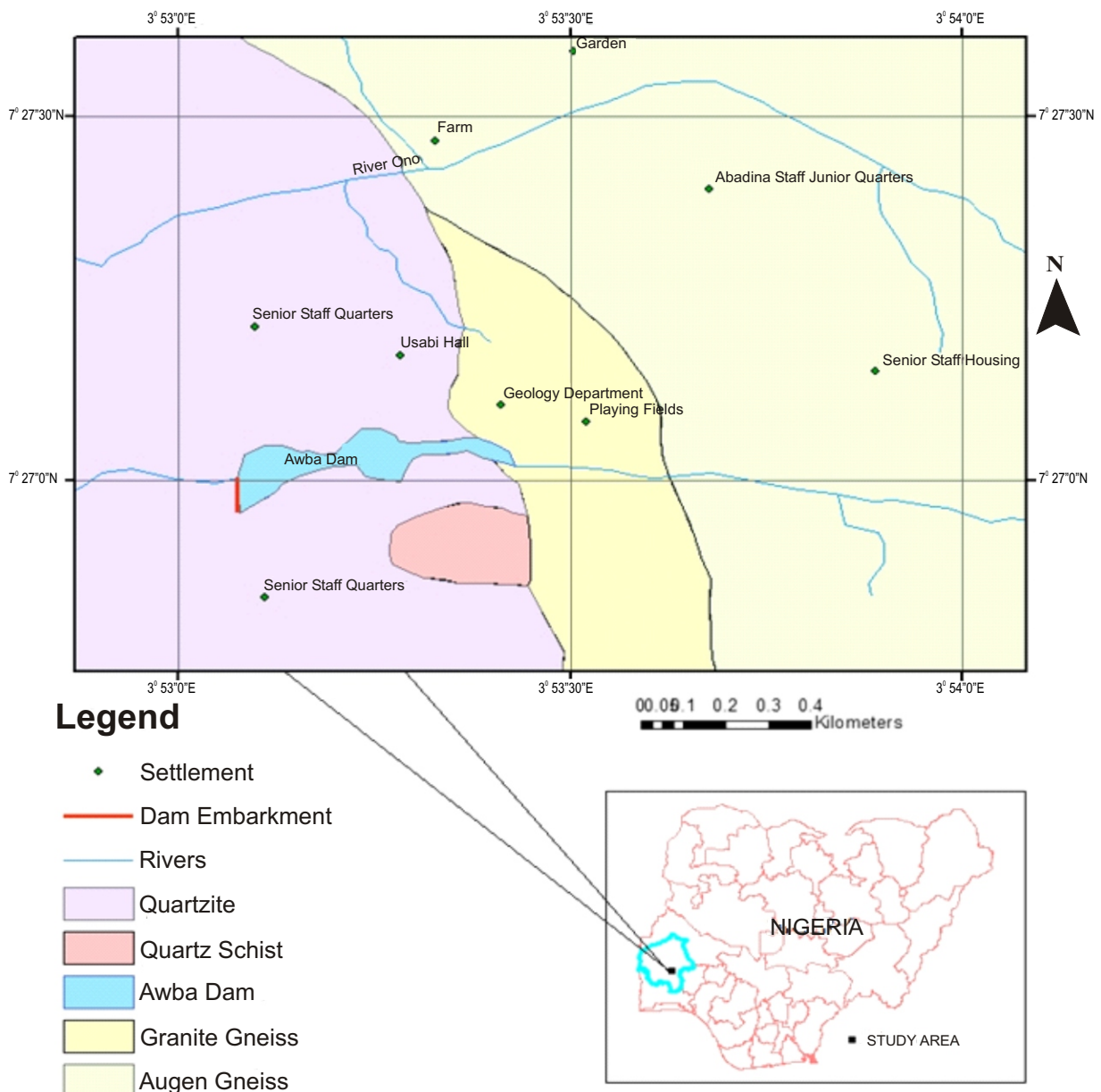


Figure 1: Geologic map of the University of Ibadan Campus (modified from Students Campus Mapping, Dept. of Geology, University of Ibadan) showing the location of the study area.

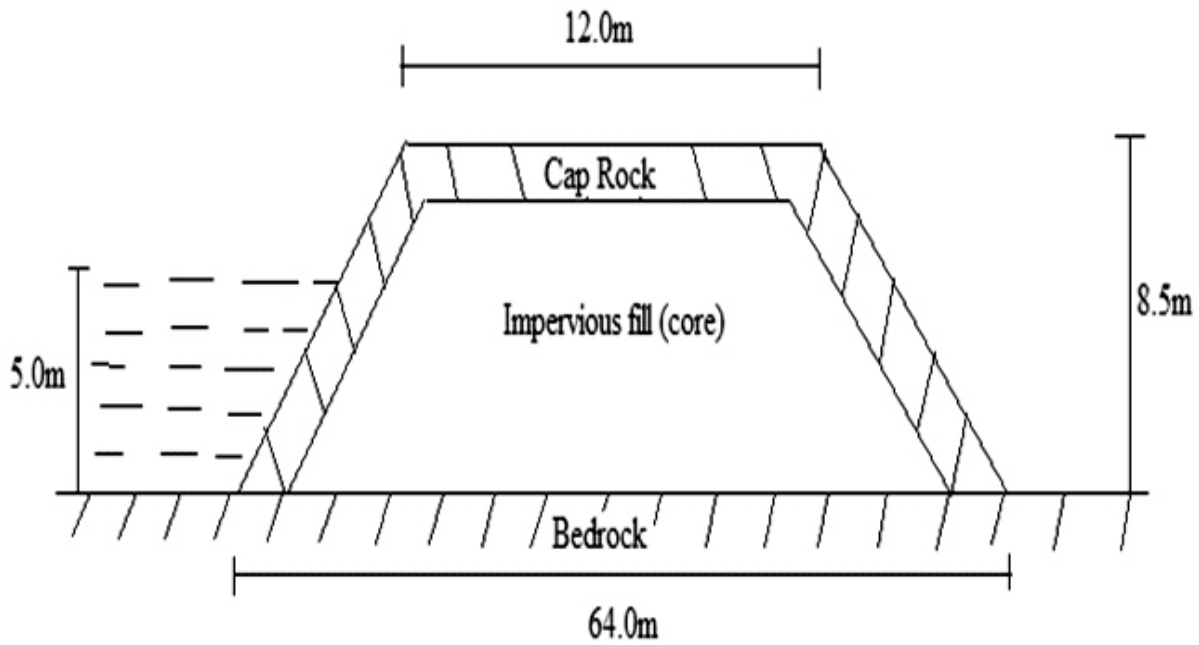


Figure 2: Awba Earth Dam Embankment Core Cross Section.

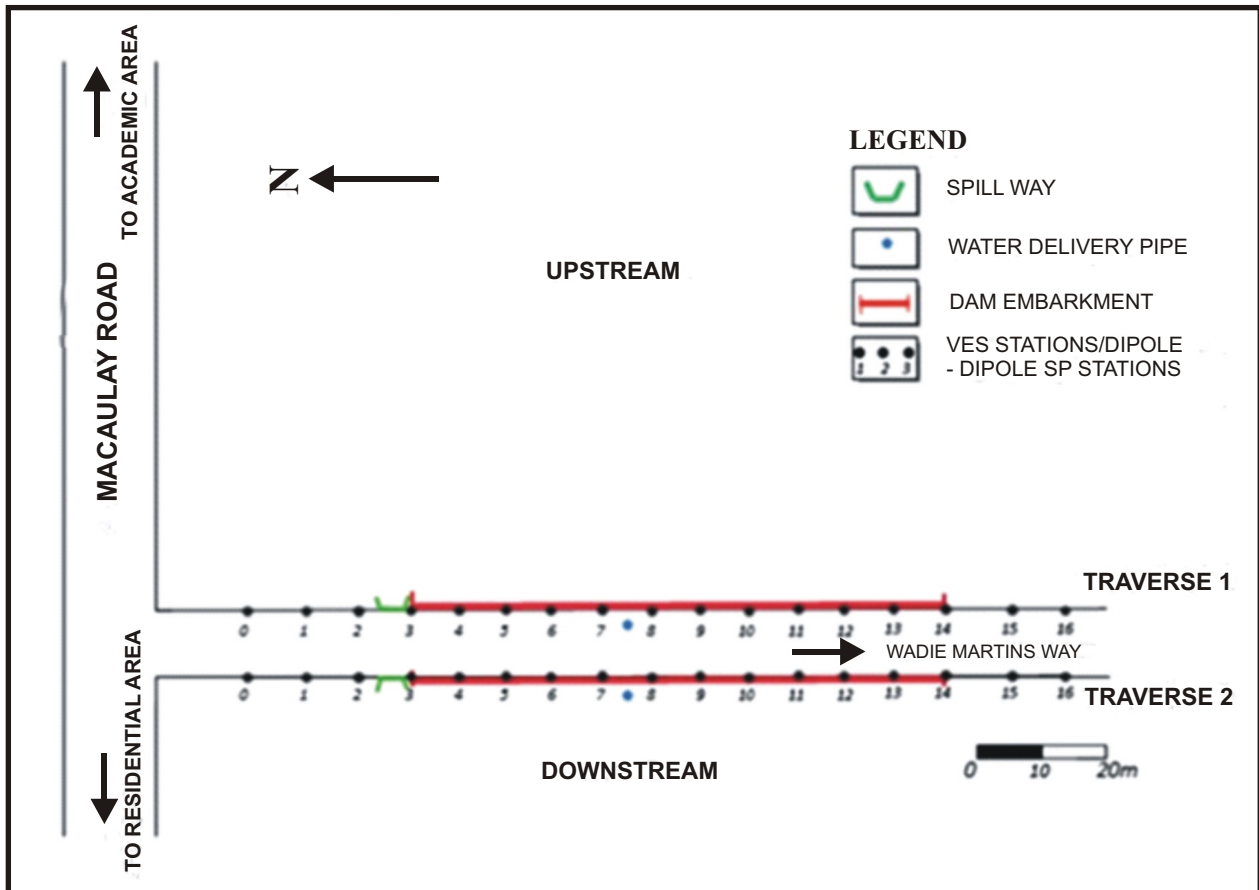


Figure 3: Site Plan of Awba Earth Dam Embankment Geophysical Stations

Physiography, Geology, Drainage, Climate and Vegetation of the Study Area

The topography of the site is gently undulating with elevation of between 190 m along the river channel and 230 m on the surrounding slopes that roll gently towards the river. The dam reservoir is underlain by quartzite outcrops which are evident

in the immediate vicinity of the dam. Other rock types within the campus are: Quartzite Schist, Augen Gneiss and Granite Gneiss (Rahaman, 1989) (Fig 1). The drainage pattern within the area is dendritic. There are two distinct seasons in the study area. The rainy season is characterized by high rainfall between April and October with a

mean annual rainfall of about 1237mm. The dry season (November-March) is characterized by dry dust originating from the Sahara desert with occasional low rainfall. Average temperature reaches a peak of 28.8°C in February and about 24.5°C in August. The entire Ibadan area falls within the rain forest region of Nigeria. The vegetation comprises of herbs, grasses and light forest, most of which are evergreen. Such trees are common along the major roads within the Campus.

METHOD OF STUDY

Geoelectrical Measurement

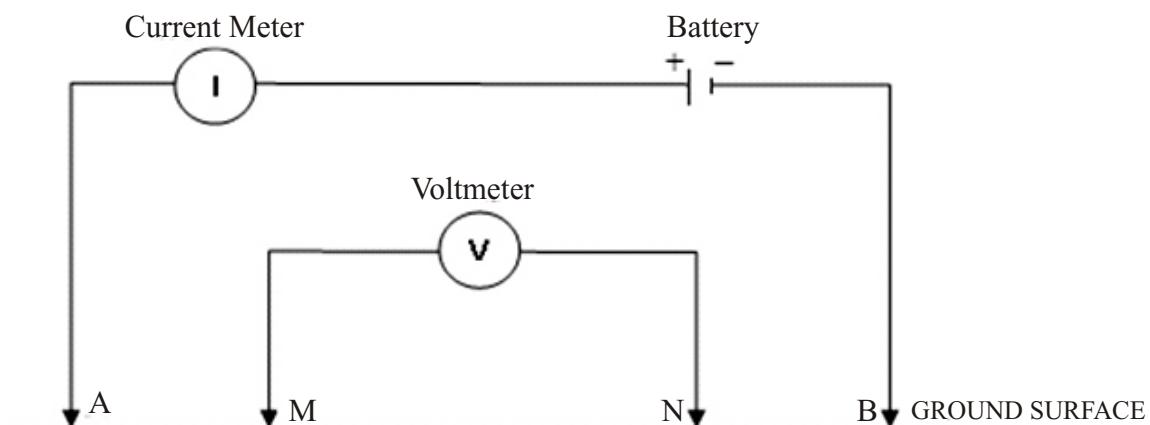
Electrical resistivity surveys are usually designed to measure the electrical resistivity of subsurface materials by making measurements on or within the earth (Abdel-Azim, *et al.*, 1996). An electrical field is imposed on the study area by a pair of electrodes at varying spacing expanding symmetrically from a central point (Fig. 4a), while measuring the surface expression of the resulting potential field with an additional pair of electrodes at appropriate spacing. For an array of current electrodes, A and B, and potential electrodes, M and N, the resistivity, is expressed by the equation:

$$\rho = \frac{2}{\left(\frac{1}{AM} + \frac{1}{BM} + \frac{1}{AN} + \frac{1}{BN}\right)} \frac{V}{I} \quad (1)$$

where I is the current introduced into the earth, V is the potential difference between the potential electrodes and AM, BM, AN and BN are inter-electrode spacings (see Fig. 4a). As long as the electrode spacing is kept constant, this equation is independent of the positions of the electrodes and is not affected when the current and potential electrodes are interchanged. Thus, with equation

(1), it is possible to determine the true resistivity of a homogenous earth medium. However, when the material constituting the medium is not constant throughout, such as in the case of the earth, the effective resistivity as computed from equation (1) will vary with the position of electrodes. In such situation, the value given in equation (1) is called the apparent resistivity and the variation in readings allows distinguishing one type of subsurface material from another. Three different field techniques are employed in resistivity prospecting. These are (1) Horizontal Resistivity Profiling (HRP) (2) Vertical Electrical Sounding (VES) and (3) Combine HRP and VES or 2D Imaging technique. The VES and the 2-D Imaging technique were adopted in this study.

In the VES technique, the potential electrodes remain fixed for a while, while the current-current electrode spacing is expanded symmetrically about the centre of the spread. When the ratio of the distance between the current electrodes to that between the potential electrodes becomes too large, the potential electrodes is displaced outwards otherwise the potential difference becomes too small to be measured accurately. The common electrode arrays suitable for VES work are the Wenner and Schlumberger arrays. The Wenner array has four electrodes positioned such that the spacing between two adjacent electrodes is one-third, whereas in the Schlumberger array the spacing between the potential electrodes must not exceed two fifth (i.e. 40%) of half the distance of the spacing (AB) of the current electrodes (Adewumi and Olorunfemi, 2005). However, the Schlumberger array (Fig. 4b) has a number of advantages over Wenner that justify its use in the present study. Among the advantages are: (1) that fewer



(a)

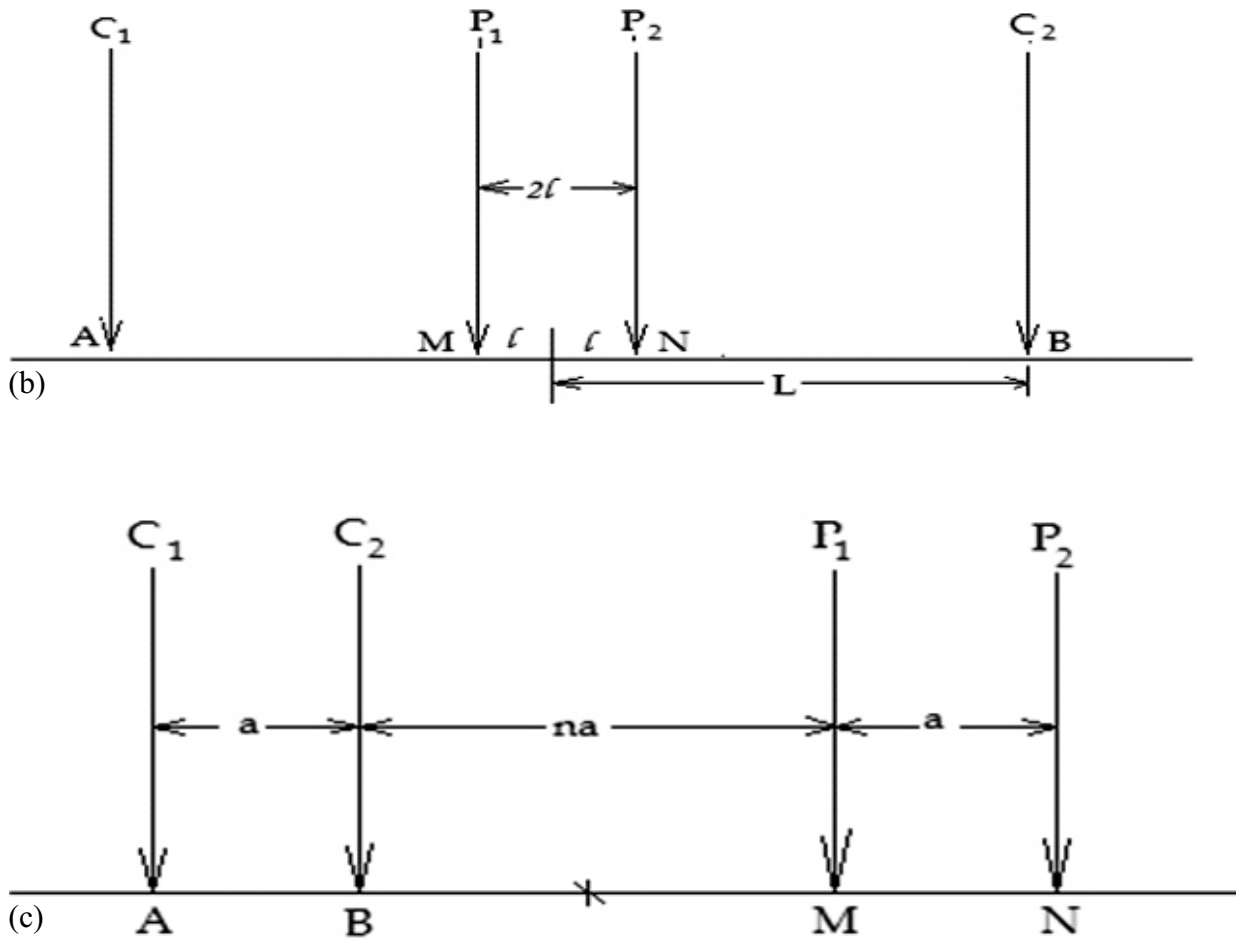


Figure 4: (a) Schematic Diagram of a Four Electrode System for Resistivity Survey (b) The Schlumberger Electrode Array (c) The Dipole-Dipole Array.

movement of the electrodes are needed than with the Wenner array; (2) lateral variations cause greater errors when potential electrodes are moved than when the current electrodes are moved; and (3) the duplication of readings with the same values of half current electrode spacing ($AB/2$) but different values of potential electrode spacing ($MN/2$) also allows an approximate correction to be made for the effects of lateral variation. For Schlumberger Array, the apparent resistivity (ρ_a) is obtained from the equation:

$$\rho_a = \frac{RL^2}{2l} \quad (2)$$

Where, ρ_a is the apparent resistivity (ohm-m), R is the ground resistance (ohm), $L (= \frac{AB}{2})$ is half the current-current electrode spacing (m), $l (= \frac{MN}{2})$

is half the potential-potential electrode spacing (m) and p is a constant ($\frac{2}{7}$).

2-D Imaging

The combined HP and VES technique involves the measurement of lateral and vertical variations in apparent resistivity of the subsurface earth. Field measurements are plotted against the points of intersection of two 45° inclined lines from the mid points of the current and potential dipoles. The common electrode configurations that are used include Wenner array, Pole Dipole array and Dipole Dipole array. In this study, the Dipole-Dipole array (Fig. 4c) was used.

SP Measurement

The equipment needed for an SP survey consists of non-polarizable electrodes. Each electrode consists of a metal rod immersed in a saturated solution of its own salt. A common arrangement is a copper rod immersed in copper sulphate ($CuSO_4$) solution contained in ceramic porous pot which allows the electrolyte to leak slowly through its porous walls, thereby making electrical contact with the ground. Two field techniques are commonly used. The gradient/fixed electrode method and the total field/fixed base techniques. The gradient technique employs a fixed separation

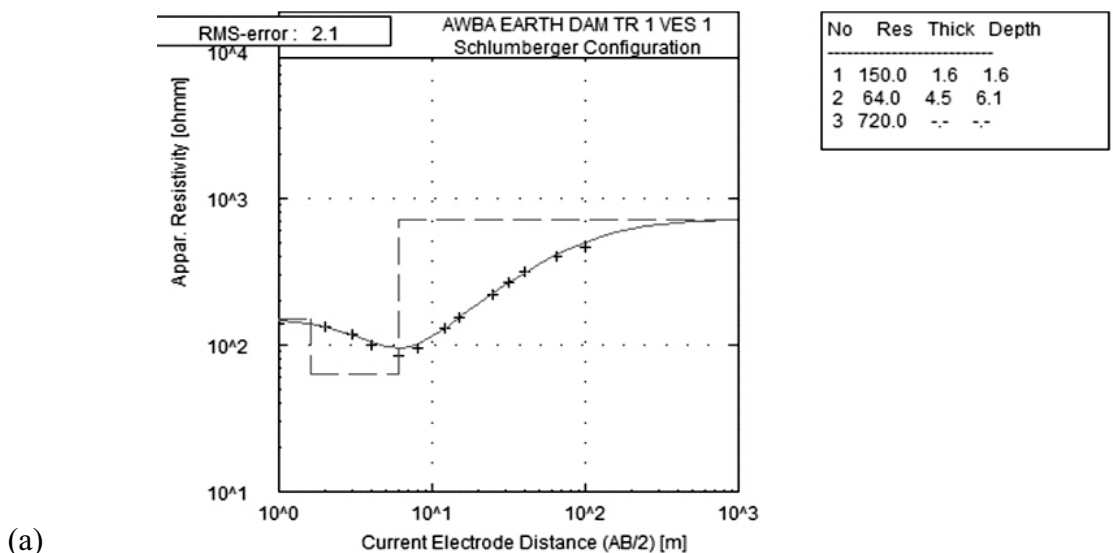
between the electrodes. The potential difference is measured between the electrodes, and then the pair is moved after each measurement with the trailing electrode occupying the position previously occupied by the leading electrode. The total potential at a measurement station relative to a base station electrode is found by summing up the incremental potential differences. Some electrode polarization is unavoidable, even with non-polarizable electrodes. This gives rise to small errors in each measurement and these add up to a cumulative error in the total potential which is taken care of by using the leap frog technique which involves interchanging the leading and trailing electrodes. The technique has the advantage of a short length of connecting wire which must be moved along the electrodes and also is suitable for prospecting in rugged terrain. However, the total field/fixed base technique utilizes a fixed electrode at a base station outside the area of exploration and a mobile measuring electrode. With this technique, the total potential is measured directly at each station. The total field technique results in smaller cumulative error than the gradient method. It allows more flexibility in placing the mobile electrode and usually gives data of better quality. Hence, the total field technique which was used in this study is usually preferred, except in difficult terrain.

The subsurface image beneath the dam embankment was achieved through integrated electrical methods of geophysical prospecting involving the Schlumberger Vertical Electrical Resistivity Sounding (VES), Dipole-Dipole resistivity 2-D imaging and the Self Potential (SP) methods. All measurements were carried out along two, N-S trending, 170 m long geophysical traverses established along the crest of the 110 m

long dam embankment (See Fig. 3). Thirty two VES stations were located at 10 m intervals while 34 dipole-dipole and SP stations at 10 m intervals were established along the traverses using inter traverse spacing of 10 m. The Campus Ohmega Terrameter was used for the resistivity and SP data measurement. The electrode spacing was varied from 1 to 100 m in the VES data acquisition. For the dipole-dipole profiling, the expansion factor, n , was varied from 1 to 5 with a depth range of 2.9 to 6.8 m (Roy and Apparao, 1971).

Data Presentation

The VES data obtained were plotted on log-log paper. The representative type curves (Fig. 5 (a) - (d)) obtained along Traverses 1 and 2 respectively were interpreted quantitatively using the partial curve matching and computer assisted 1-D forward modelling. This interpretation of the VES data in terms of subsurface layering was based on geoelectric equivalence of an idealized embankment section (See Fig. 2) in which a low resistivity, impervious clay core (or fill) occurs between a more resistive caprock and competent bedrock (e.g. Olorunfemi *et al.*, 2000a). The WinResist computer 1-D forward modeling software was used for refining the partial curve matching interpreted results. Htype curves account for 97% of the total type curves obtained along the dam embankment while the HKHtype constitutes 3%. Detail depth sounding interpretation results obtained for the thirty two (32) VES stations are as presented in Table 1. The results were used to construct 2-D geoelectric sections (Figs. 6 (a) and (b)). The dipole-dipole data were inverted into 2-D resistivity images (Figs. 7 and 8 (a)-(c)) using the DIPPRO™ 4.0 inversion software. The SP data were presented as profiles (Figs. 9 (a) and (b)).



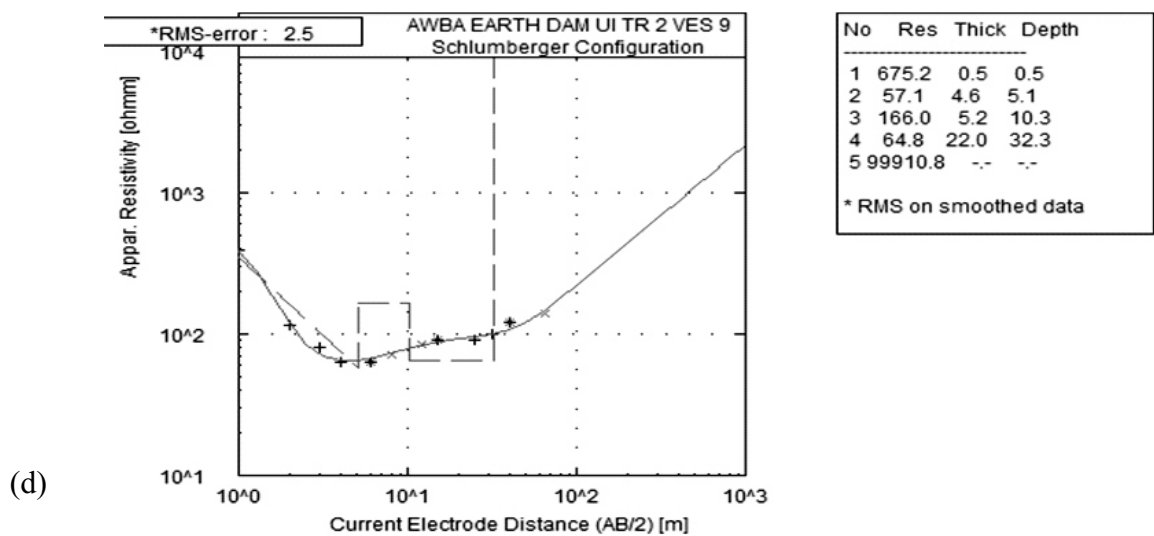
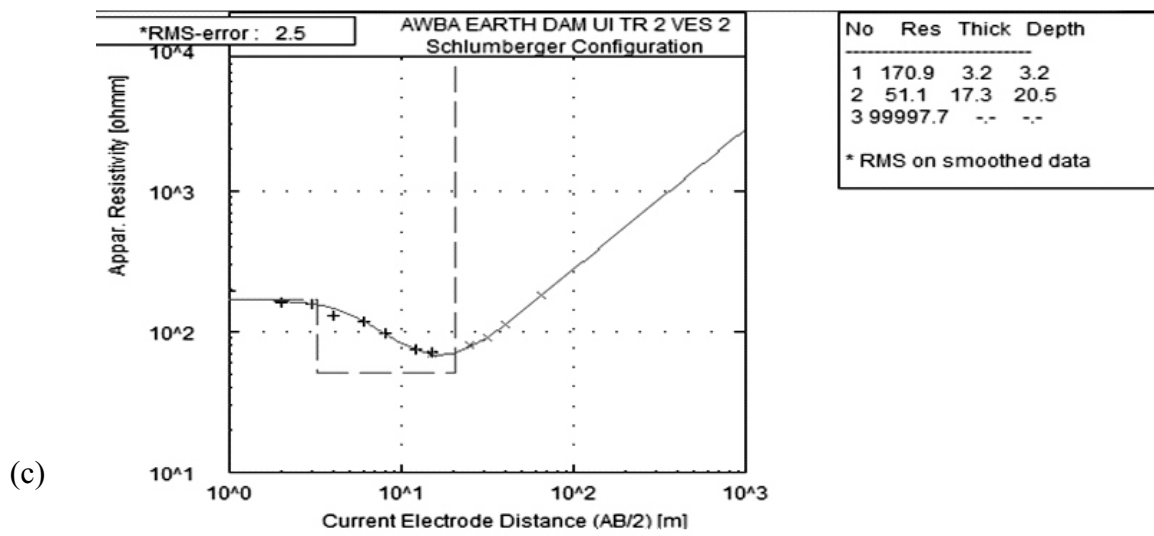
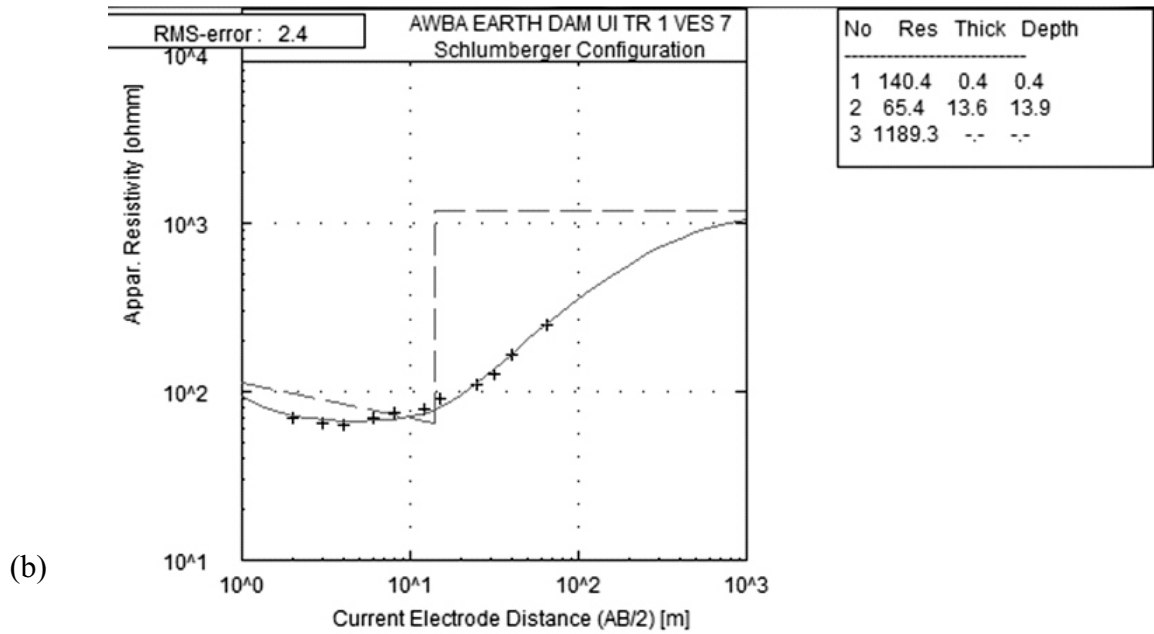
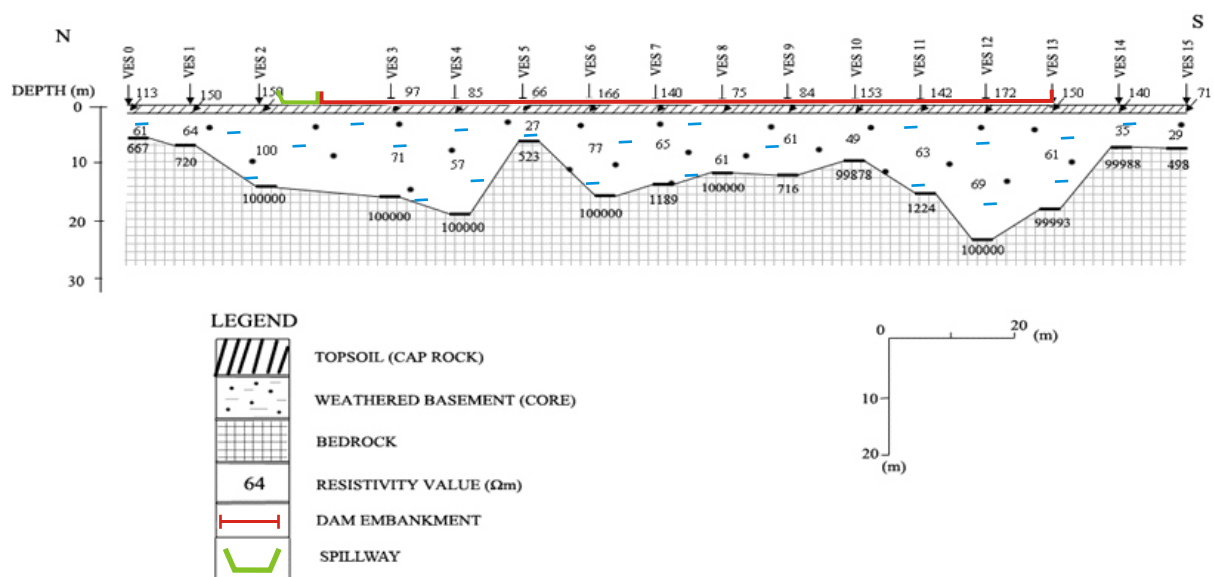


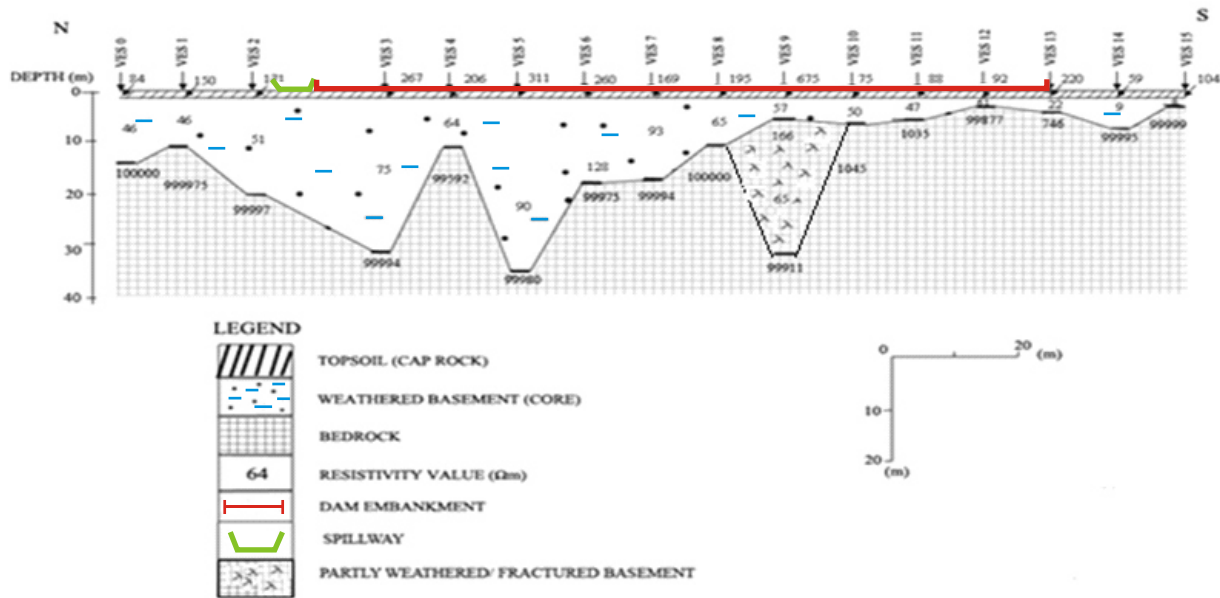
Figure 5: Typical Depth Type Curves obtained from Awba Dam Embankment.

Table 1: Depth Sounding Interpretation Results

VES Station	TRAVERSE 1			TRAVERSE 2		
	Resistivity (ohm-m) $\rho_1/\rho_2/\dots/\rho_n$	Depth (m) $D_1/D_2/\dots/D_n$	Type curve	Resistivity (ohm-m) $\rho_1/\rho_2/\dots/\rho_n$	Depth (m) $D_1/D_2/\dots/D_n$	Type curve
0	113/61/667	1.1/5.6	H	84/46/100000	1.7/13.9	H
1	150/64/720	1.6/6.1	H	150/46/99975	0.9/11.1	H
2	150/100/100000	0.6/14.4	H	171/51/99998	3.2/20.5	H
3	97/71/100000	0.6/14.7	H	267/75/99995	1.6/31.6	H
4	85/57/100000	1.7/18.7	H	206/64/99592	1.6/11.1	H
5	66/27/523	1.4/5.5	H	311/90/99980	0.7/35.3	H
6	166/77/100000	0.4/16.4	H	260/128/99975	0.8/17.7	H
7	140/65/1189	0.4/13.9	H	169/93/99994	1.7/17.6	H
8	75/61/100000	1.0/12.0	H	195/65/100000	0.5/11.5	H
9	84/61/716	0.9/12.3	H	675/57/166/65/99911	0.5/5.1/10.3/32.3	HKH
10	153/49/99879	1.9/9.8	H	75/50/1045	0.8/6.8	H
11	142/63/1225	1.5/15.5	H	88/47/1035	1.0/6.0	H
12	172/69/100000	2.0/24.6	H	92/60/99877	0.6/3.6	H
13	150/61/99993	2.0/18.1	H	221/23/746	0.3/4.8	H
14	140/35/99988	0.6/7.2	H	59/09/99995	0.8/8.5	H
15	71/29/498	0.7/7.3	H	104/08/100000	0.7/3.2	H



(a)



(b) Figure 6: Geoelectric 2-D Image along Awba Earth Dam Embankment.
 (a) Along Traverse 1 (Up Stream) (b) Along Traverse 2 (Down Stream)

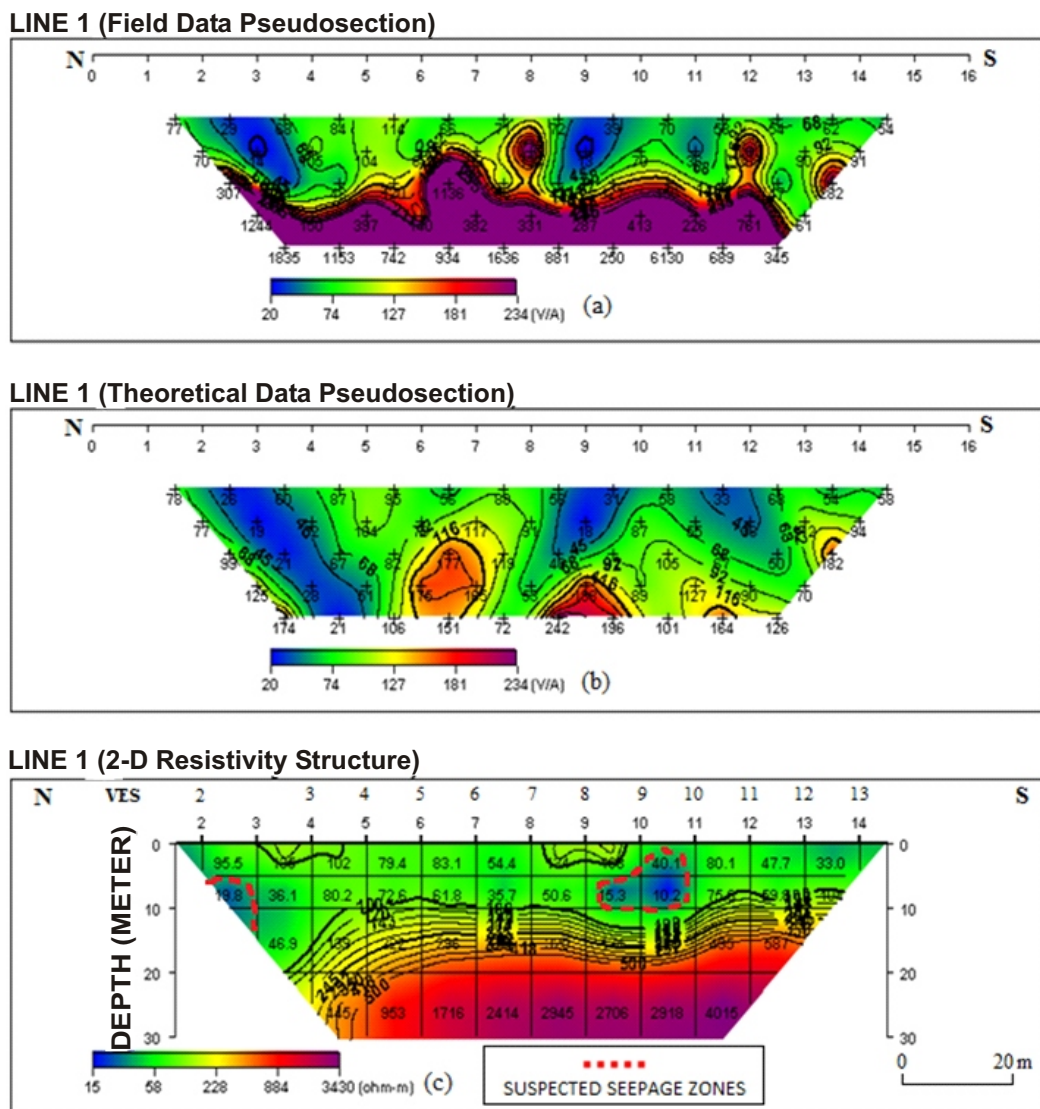
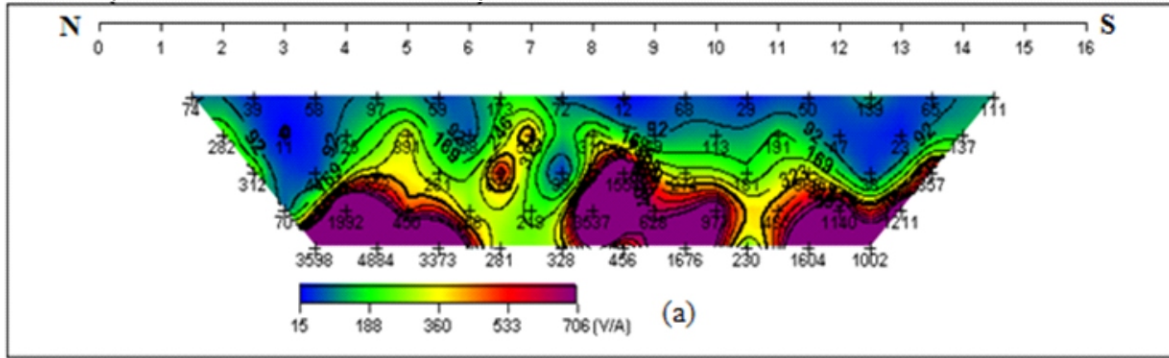
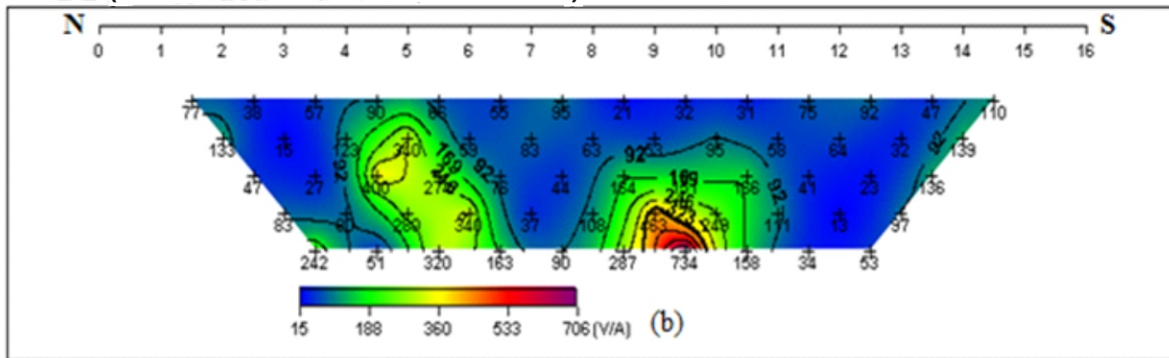


Figure 7: (a) Observed Dipole-Dipole Pseudosection (b) Theoretical Pseudosection and (c) 2-D Inverse Model along Awba Dam Embankment Traverse 1(Up Stream).

LINE 2 (Field Data Pseudosection)



LINE 2 (Theoretical Data Pseudosection)



LINE 2 (2-D Resistivity Structure)

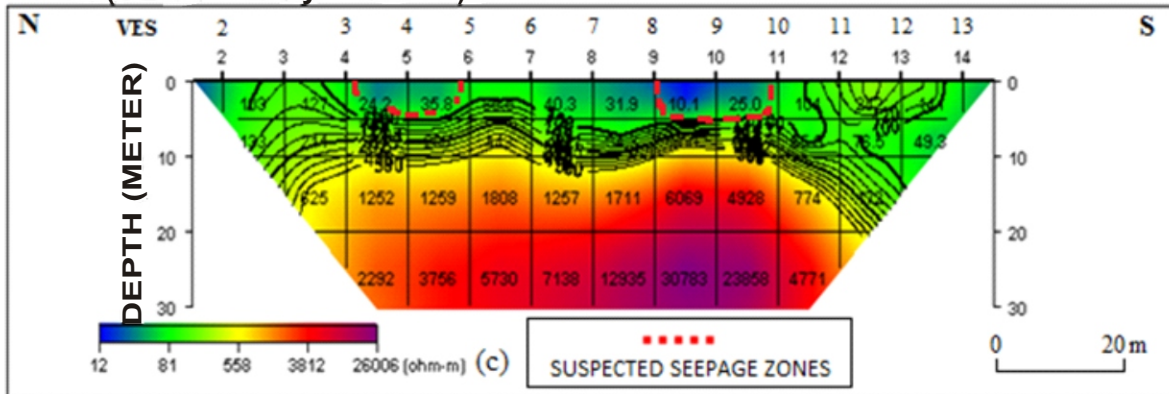
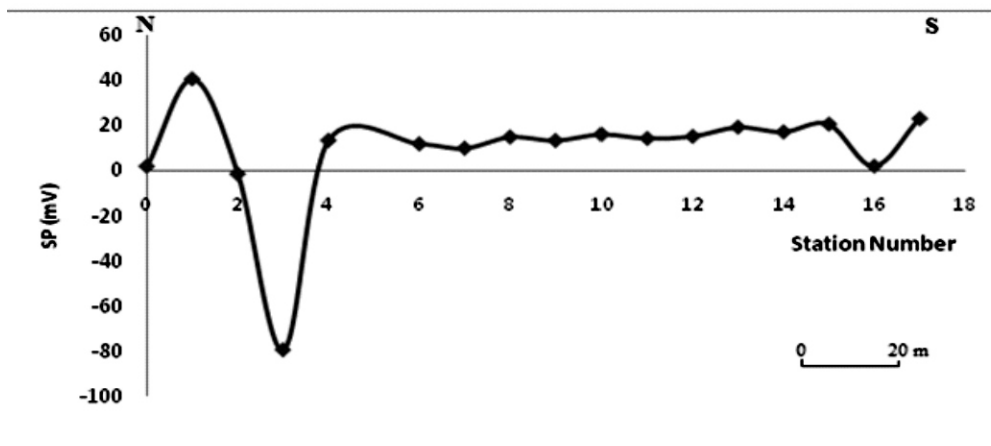
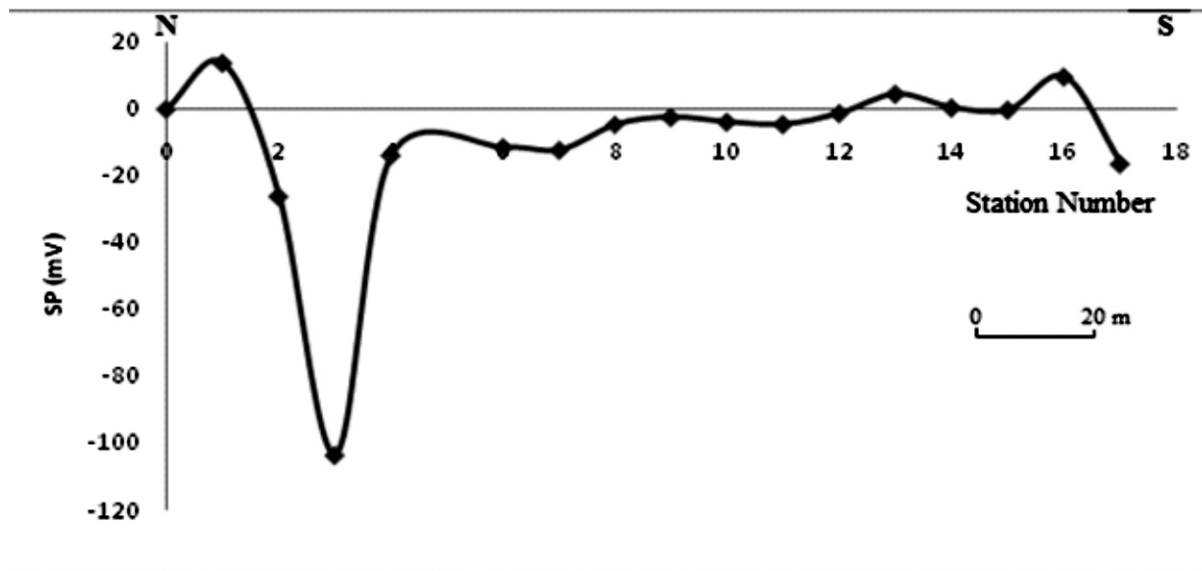


Figure 8: (a) Observed Dipole-Dipole Pseudosection (b) Theoretical Pseudosection and (c) 2-D Inverse Model along Awba Dam Embankment Traverse 2 (Down Stream).



(a)



(b)

Figure 9: Total Field Self Potential Profile along Awba Dam Embankment.

(a) Along Traverse 1 (With Reference to Up Stream)

(b) Along Traverse 2 (With Reference to Down Stream)

RESULTS AND DISCUSSION

The geoelectric section (Fig. 6a) along Traverse 1 displays three distinct geologic layers. These layers are interpreted as a top clay/sandy clay (cap rock) layer with layer resistivity and thickness values of 66 - 172 ohm-m and 0.4 - 2.0 m respectively overlying a clay core/weathered layer with layer resistivity and thickness ranges of 29 - 100 ohm-m and 5.5 - 24.6 m respectively. The water level in the dam lake falls within this second layer and is hence characterized by low layer resistivity values due to high moisture content. The third layer is the presumably fresh basement bedrock with layer resistivity values of between 498 and 100000 ohm-m. The geoelectric section (Fig. 6b) along Traverse 2 displays three distinct geologic layers. These layers are the clay/sandy clay/laterite (cap rock) with layer resistivity and thickness values of 59-675 ohm-m and 0.3-3.2 m respectively, clay/sandy clay core/weathered layer with layer resistivity and thickness range of 8-166 ohm-m and 3.2-35.3 m respectively. The third layer is the presumably fresh basement bedrock with layer resistivity range of between 746 and 100000 ohm-m. The 2-D resistivity structure (Fig. 7c) along Traverse 1 displays two anomalously low resistivity zones with values of less than 45 ohm-m suspected to be seepage zones (Olorunfemi *et al.*, 2004) along the Traverse 1 (Up Stream). These suspected seepage zones are located between stations 2 and 3 (20 - 30 m) at about 8 m depth and between stations 9 and 11 (90 - 110 m) at depth range of between 4 and 10 m within the dam embankment. Figure 8c displays

the 2-D resistivity structure along Traverse 2 Down Stream of the dam embankment. The presumably seepage zones are delineated between stations 4 and 6 (40 - 60 m) and 9 and 11 (90 - 110 m) along the traverse at depths of less than 5 m. The latter suspected seepage zone falls within the delineated zone along Traverse 1. The Total Field SP profile along Traverse 1 (Fig. 9a) shows one major peak negative anomaly (-80 mV) between stations 2 and 4 (20 - 40 m). Similarly, Traverse 2 (Fig. 9b) shows such major peak negative anomaly (-104 mV) between same stations. These anomalies are diagnostic of the metallic bleeding pipe concealed between the spillway and the dam embankment.

CONCLUSIONS

Electrical imaging of the Awba earth dam embankment was carried out with the aim of identifying the possible seepage zones within the embankment. The vertical electrical sounding, dipole-dipole horizontal profiling and total field Self Potential profiling were employed. The geoelectric sections revealed three distinct geoelectric layers. These horizons include the topsoil (cap rock) of clay/sandy clay, the core/weathered layer made up of wet clay and the fresh basement bedrock. The 2-D resistivity structure revealed that the core of the dam embankment is characterized by low resistivity zones between stations 2 and 3 (20 - 30 m) at about 8m depth and between stations 9 and 11 (90 - 110 m) at a depth range between 4 and 10 m within the

dam embankment along Traverse 1. Low resistivity zones were also encountered between stations 4 and 6 (40 - 60 m) and 9 and 11 (90 - 110 m) at depth range between 0 and 5 m along Traverse 2. With an embankment height of 8.5 m, these are evidences of probable seepages within and beneath the core. The Total Field SP profile revealed one anomalous zone along traverses 1 and 2. The major anomaly occurred between stations 2 and 4 (20 - 40 m) and is diagnostic of a metallic bleeding pipe concealed between the spillway and the dam embankment.

REFERENCES

- Abdel-Azim, M.E, Mahmoud, M.S and Kamal, A.D. 1996. Geoelectrical and Hydrogeochemical Studies for Delineating Groundwater Contamination due to Salt-Water Intrusion in the Northern Part of the Nile Delta, Egypt. *GROUNDWATER*, 35, (2), 218.
- Adewumi, I and Olorunfemi, M.O. 2005. Using Geoinformatics in Construction Management. *Journal of Applied Sciences* 5(4). 761-767, ISSN 1812-5654.
- Bogoslovsky, V.A and Ogilvy, A.A 1970. Natural Potential Anomalies as a quantitative index of the rate of water seepage from reservoir. Hydrogeological investigation. Proceedings of the symposium of the application of geophysics to engineering. *Geophysical Prospecting*, 18, 262-268.
- Butler, D.K., Llopis, J.L. and Deaver, C.M. 1988. Comprehensive Geophysical Investigation of an Existing dam foundation. *Geophysics*, the Leading Edge of exploration. August, 1988, 10-18.
- Christensen, N.R. and Sorensen, K.I 1994. Integrated use of electromagnetic methods for Groundwater and Environmental problems. Proceedings of the Symposium on the Application of Geophysics to Environmental and Engineering Problems SAGEEP, 163-176.
- Erchul, R.A. and Slifer, D.W. 1987. The use of Spontaneous Potential in the detection of Groundwater flow patterns and flow rate in Karst areas, Proceedings Multidiscipline Conference on Sinkholes and the Environmental Impacts of Karst : 2, 2217 226.
- Haines, B.M. 1978. The detection of water leakage from dams using streaming potentials: Transaction of the SPWLA Annual Logging Symposium, Issue 19.
- Lowrie, W. 1997. Fundamentals of Geophysics. Cambridge University Press. The Edinburgh Building, Cambridge CB2 2RU, United Kingdom, 208.
- McLean, A.C. and Gribble, L.O. 1997. Geology for Civil Engineers. George Allen and Unwin. 34-45.
- Olorunfemi, M.O., Ojo, J.S., Sonuga, F.A., Ajayi, O. and Oladapo, M.I. 2000a. Geoelectric and Electromagnetic Investigation of the Failed Koza and Nassarawa Earth Dams around Katsina, Northern Nigeria. *Journal of Mining and Geology*, 36(1), 51-65.
- Olorunfemi, M.O., Ojo, J.S., Sonuga, F.A., Ajayi, O. and Oladapo, M.I. 2000b. Geophysical Investigation of Karkarku earth dam Embankment. *Global Journal of Pure and Applied Sciences*. 6, (1), 117-124.
- Olorunfemi, M.O., Idornigie, A.I., Fagunloye, H.O. and Ogun, O.A. 2004. Assessment of Anomalous Seepage Conditions in the Opa Dam Embankment, Ile-Ife, Southwestern Nigeria. *Global Journal of Geological Sciences*. 2, (2), 191-198.
- Payne, K.M. and Corwin, R.F. 1999. Self Potential Methods to Investigate the Water Seepage Flow through Earthfill Embankment Dams. Proceedings of the Symposium on the Application of Geophysics to Environmental and Engineering Problems (SAGEEP), 4148.
- Roy, A. and Apparao, A. 1971. Depth of Investigation in direct current methods. *Geophysics*. 36, 943-959.
- Rahaman, M.A. 1989. Review of the Geology of Southwestern Nigeria. In *Geology of Nigeria*, 2nd Edition, (Kogbe, C.A., ed), Rock View (Nig.) Ltd., Jos Nigeria.
- Sjodahl, P. 2006. Resistivity Investigation and Monitoring for detection of Internal Erosion and Anomalous and Seepage in Embankment Dams, Doctoral Thesis, ISRN LUTVDG / TVTG 1017 SE, ISBN 978-91-973406-5-6, Lund University, Lund. Pp.86.

Ife Journal of Science
Table of Contents: December 2011 Edition; Vol. 13, No. 2

Jegede, O.I. and Fawole, O.O. ,	Fecundity and Egg Size Variation in <i>Tilapia Zillii</i> (gervais) and <i>Tilapia Mariae</i> (boulenger) from Lekki Lagoon, Nigeria.	219
Bayowa, O.G., Ilufoye, D.T. and Animasaun, A.R. .	Geoelectric Investigation of Awba Earth Dam Embankment, University of Ibadan, Ibadan, Southwestern Nigeria, for Anomalous Seepages.	227
Adedeji A.A., Aduwo A. I., Aluko O. A. and Awotokun F.	Effect of Chicken Droppings as Organic Fertilizer on Water Quality and Planktonic Production in an Artificial Culture Media	239
Aborisade, Abiola T and Adebo, Cosmas T	Effect of Curing on the Shelf Life of Ambersweet Oranges (<i>citrus Sinensis</i> Osbeck) Stored at Ambient Tropical Condition	251
Ogungbesan G.O. and Akaegbobi I.M.	Petrography and Geochemistry of Turonian Eze-aku Sandstone Ridges, Lower Benue Trough, Nigeria Implication for Provenance and Tectonic Settings.	263
Ayinde F.O. and Asubiojo O.I.	Micellar Catalysis of the Hydrolysis of Aryltrifluoroacetates	279
Eze, U.N., Okonji, R.E., Ibraheem, O. and Shonukan, O.O.	Isolation And Characterization Of A Bacterial Thermostable Protease From Poultry Dung.	289
Badejo M.A, Owojori O.J., and Akinwole P.O.	A Survey of the Population of the African Weaver Ant, <i>Oecophylla Longinoda</i> (hymenoptera:formicidae) in Contrasting Habitats in Ile-Ife, South-Western Nigeria.	299
S. A. Opeloye	Depositional Environment of Lamja Sandstone in the Upper Benue Trough, Northeastern Nigeria	309
Okunlola, A.O., Akinola, O.O. and Olorunfemi, A.O.	Petrochemical Characteristics and Industrial Features of Talcose Rock in Ijero-Ekiti Area, Southwestern Nigeria.	317
Adekoya, J.A., Aluko, A.F. and Opeloye, S.A.	Sedimentological Characteristics of Ajali Sandstone in the Benin Flank of Anambra Basin, Nigeria	327
Jimoh, M.A., Saheed, S.A. and Botha, C.E.J.	Response of Barley Cultivars to Infestations of the Two South African Biotypes of the Russian Wheat Aphid	339
Omafuvbe, B.O. , Feruke-Bello, Y.M. and Adeleke, E.O.	Aerobic Mesophilic Bacteria Associated with Irish Potato (<i>solanum Tuberosum</i> L.) Spoilage and their Susceptibility Pattern to Lactic Acid Bacteria and Antibiotics.	347
Oluyemi, E.A. and Olabanji, I.O.	Heavy Metals Determination in Some Species of Frozen Fish Sold at Ile-Ife Main Market, South West Nigeria	355
Oketayo, O.O. and Ojo, J.O.	Anthropometric Predictive Equations for Percentage Body Fat in Nigerian Women Using Bioelectrical Impedance as Reference	363
Oluduro A. O., Bakare M. K., Omoboye O. O., Dada C.A. and Olatunji C. I.	Antibacterial Effect of Extracts of <i>Acalypha Wilkesiana</i> on Gastrointestinal Tract Pathogens and Bacteria Causing Skin Infections in Neonates.	371
Adeleke, E.O., Omafuvbe, B.O., Adewale, O.I. and Bakare, M.K.	Screening and Isolation of Thermophilic Cellulolytic Bacteria from Cocoa Pod and Cassava Peel Dumpsites in Ile-Ife, Southwest Nigeria	381
Akinola, A. P. Borokinni, A. S. Fadodun, O. O. Olokuntoye, B. A.	Finite Element Modeling of Deformation in a Composite Bar	389